Research Article

Title: Visual modelling validates prey detection by means of diurnal active photolocation in a small cryptobenthic fish

Running Title: Modelling active photolocation

Authors: Pierre-Paul Bitton (Corresponding author), Sebastian Alejandro Yun Christmann, Matteo Santon, Ulrike K. Harant, Nico K. Michiels

Affiliations: Institute of Evolution and Ecology, Faculty of Science, Eberhard Karls Universität Tübingen, Auf der Morgenstelle 28, 72076 Tübingen, Germany

E-mails: Pierre-Paul Bitton: pierre-paul.bitton@uni-tuebingen.de

Word count:

Manuscript elements: Figures = 4

Tables = 0

Supplemental Information = 1 Table, and 2 Figures

Author contribution P-P.B. and N.K.M conceptualized the study. All authors collected data. P-P.B., S.Y.C. analyzed data. P-P.B., S.Y.C., and N.K.M. wrote the manuscript, and all edited the manuscript.

Author Declaration The authors declare no conflict of interest.

Keywords Foraging, Prey-Predator Interaction, Active Sensing, Vision, Spectroradiometry

Abstract

Active sensing has been well documented in animals that use echolocation and electrolocation. Active photolocation, or active sensing using light, has received much less attention, and only in bioluminescent nocturnal species. Recently, however, evidence has suggested the diurnal triplefin *Tripterygion delaisi* uses controlled iris radiance, termed ocular sparks, for prey-detection. While this form of diurnal active photolocation was behaviourally described, a study exploring the complete physical and theoretical process would provide a more compelling case supporting this mechanism. In this paper, we investigate the conditions under which diurnal active photolocation could assist *T. delaisi* in detecting potential prey items. In the field, we sampled prey gammarids (Genus *Cheirocratus*) from foraging substrates, and characterized the spectral properties of their body and eyes, which possess strong reflectors between the ommatidia. In the laboratory, we quantified ocular spark sizes and the angular dependence of their radiance. Together with environmental light measurements and the visual properties of *T. delaisi*, we modeled diurnal active photolocation under various scenarios. Our results corroborate that diurnal active photolocation can help *T. delaisi* detect gammarids at distances relevant to foraging, 4.5 cm under favourable conditions and up to 2.5 cm under average conditions. Because ocular sparks are widespread across many different fish species, diurnal active photolocation for micro-prey may be a common predation strategy.

Active sensory systems have been well studied in several animals. For example, the echolocating behavior of bats, by which the reflection of emitted sound waves contributes to navigation in the dark, was detailed starting in 1938 (1, 2), and active electrolocation, by which the disruptions of weak electrical fields are used to detect potential prey and predators, is well known from model organisms such as *Apteronotus leptorhynchus* (3, 4). In contrast, active photolocation, the process by which organisms emit light to survey their environment, seems limited to bioluminescent organisms; only deep-sea dragonfish (Fam. Stomiidae), lanternfish (Fam. Myctidae), and nocturnal flashlight fish (Fam. Anomalopidae) are assumed to use active photolocation (5-7). However, recent evidence suggests active photolocation, by means of controlled light redirection, could also be used in diurnal fish to assist in prey detection, and may be generally common across fish species (8).

Michiels et al. (8) described a mechanism that allows the triplefin *Tripterygion delaisi* to redirect ambient light by taking advantage of its laterally protruding lenses and reflective irides, and discussed how this may assist in the detection of camouflaged micro-prey. The central basis of the mechanism is that downwelling light strikes the dorsal part of the eye, is focused by the protruding lens onto the iris below the pupil, and is reflected in the horizontal plane of vision. The focussed light can be radiated by the red fluorescent section of the iris producing a 'red ocular spark', reflected by a blue-white area below the pupil generating a 'blue ocular spark' (**Fig. 1**), or turned on and off by rotating and tilting the iris (see Fig. 2 in (8)). Because downwelling light in the aquatic environment is many times more intense than sidewelling light (9, 10), blue ocular sparks appear much brighter than the background. Michiels et al. (8) emphasized that ocular sparks are too weak to illuminate an entire scene, but suggested they may be sufficiently radiant to reveal strong and/or directional reflectors in nearby target organisms.

Indeed, strongly reflecting structures are abundant in aquatic ecosystems, specifically in the eyes of both vertebrates and invertebrates (11-14). For example, camera eyes that possess either a *tapetum lucidum* or *stratum argenteum* are retroreflective, and produce the eyeshine observed when

42 illuminating nocturnal animals. This type of reflected eyeshine is only perceived if the illuminating
43 source is coaxial to the receiver's eye because most of the light is returned to the source in a narrow
44 angle. Furthermore, invertebrates such as stomatopod larvae also possess strong reflectors that can
45 function to camouflage their opaque retinas (12). Though not true retroreflectors, the reflectance of
46 marine invertebrate compound eyes is often stronger towards coaxial alignment (8, 12, 15). Strong
47 directional reflectors and coaxially generated illumination are key components of the mechanism
48 proposed by Michiels et al. (8) because the ocular sparks are generated on the irides, immediately
49 adjacent to the pupil. Thus, ocular sparks could make use of the reflectance of prey eyes to increase the
50 probability of detection, as has been suggested for nocturnal, bioluminescent species (15-17).
51 The experiment reported in Michiels et al. (8) was conducted in the laboratory and focused on
52 ocular spark modulation in response to prey presence and background hue. No studies have yet
53 explored the physical and theoretical basis of the complete process to describe the conditions under
54 which ocular sparks could assist triplefins in detecting prey under natural conditions. In this study, we
55 use simple mathematical expressions and visual modelling to determine the parameters that would
56 enable triplefins to benefit from blue ocular sparks for prey detection. In the field, we collected
57 measurements of ambient light fields and characterised the reflective properties of a background in
58 which gammarids (Crustacea: Amphipoda), important triplefin prey items (18, 19), are found. In the
59 laboratory, we measured the ocular spark properties of the triplefin and the optical properties of the
60 eyes and bodies of gammarids. Finally, we combined these data with triplefins' species-specific visual
61 system characteristics (20) to inform visual models.
62

Figure 1. *Tripterygion delaisi* with blue ocular spark. Photo credit: Nico K. Michiels

Results and Discussion

Properties of ocular sparks

Previous work showed that the relative radiance of the average ocular spark peaks around 472 nm at 2.15 times that of a diffuse white standard, and that the total area under the curve between 380 and 700 nm averaged 1.36 times that of a diffuse white standard (range 0.63 to 2.09, *n* = both eyes of 5 fish; data from (8)). To further characterize the properties of the blue ocular spark we measured its size, and its radiance at different angles in relation to a white diffuse standard under controlled light environments. The radius equivalent (area as a circular disk) of the ocular sparks ranged from 0.10 mm to 0.24 mm (mean = 0.16 mm, *n* = 10 fish). The relative radiance of the spark was similar across all angles measured along the equatorial axis (**Fig. 2**). Combined, these results suggest that the chromatophores composing the reflective patch are not strongly specular. Hence, reflectance values higher than 1 were attributed to light being focused onto an area smaller than the lens catchment area. While a narrow beam of energy increases the maximum distance of an active sensing signal, it limits the active space from which animals can gather information, leaving them 'blind' in other directions (21). Hence, directional emission would not be particularly advantageous in an active visual sensing system,

as the exact position of the reflector would have to be known. Under these circumstances, a broad active sensing signal would be useful for scanning a large area of the visual environment for strong directional reflectors.

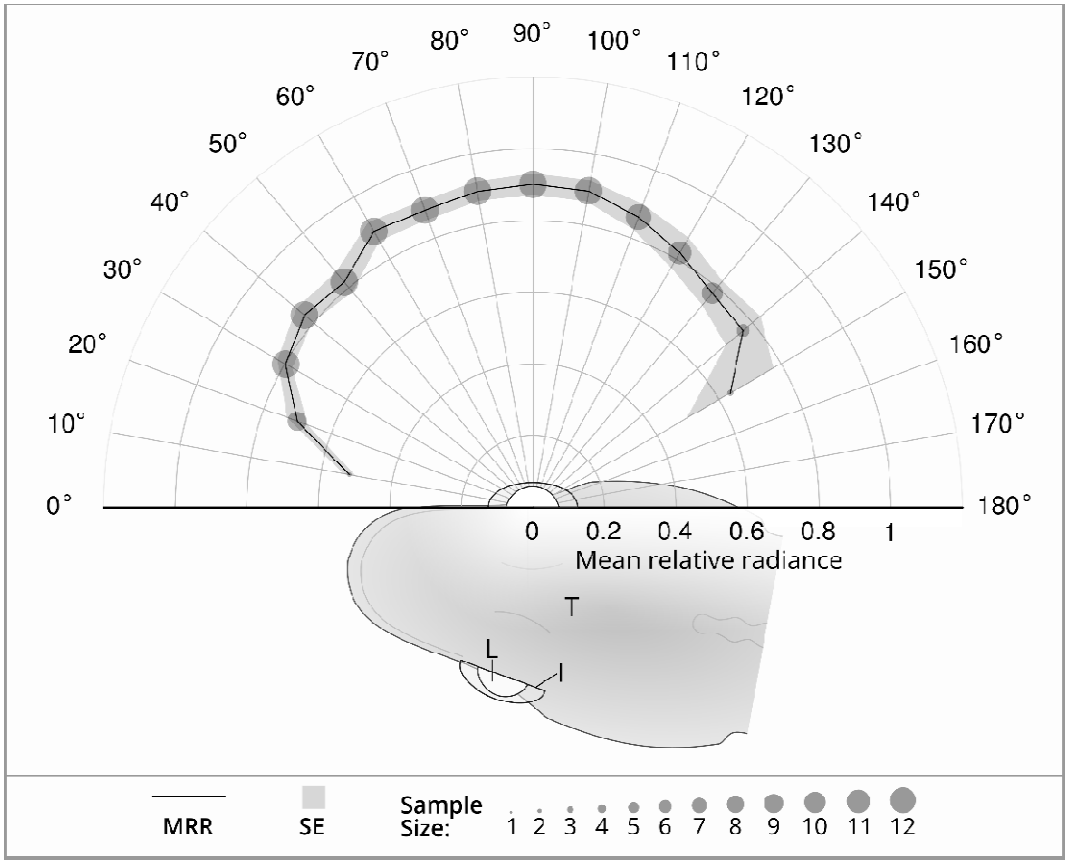

Figure 2. The mean relative radiance (MRR) of the blue ocular spark does not vary along the equatorial axis. MRR is represented by the solid line, the corresponding standard error (SE) by the light grey area, and the sample size of each measured angle by the size of the discs. Fish is seen from a dorsal perspective and naming scheme for angles in relation to the iris of *Tripterygion delaisi*: 90° = normal angle, 0° = angle parallel at the anterior start of the semi-circle and 180° at the posterior end. T = *T. delaisi* body, I = Iris, L = Lens.

Spectral properties of Cheirocratus *gammarids*

Our measurements on gammarids eyes (*Cheirocratus* sp.) were collected from the entire compound eye, which is generally reflective in decapod shrimps (15). Focus stacking images revealed the reflective units of gammarid eyes are not found in the optical pathway of the eye (**Fig. 3**), but appear to be between ommatidia akin to those described in *Pullosquilla thomassini*, *Pseudosquillana richeri*, and *Harpiosquilla sp.* (12). While these reflectors would not improve vision in dim light as other reflectors do (22) , they would help camouflage the gammarid eye (12). We measured the reflection and transmission spectra of gammarid body and eyes using a spectroradiometer coupled to a compound microscope (see Methods section for details) under 10 × 10 magnification (n = 19). On average, the body of the gammarids transmitted more light than they reflected, which would make them well camouflaged against any background (**Fig. 3**). Overall eye reflectance, within the 400 to 700 nm wavelength range and illuminated with a coaxial light source (epi-illumination), was on average 4.09 times greater than when illuminated with a light source set at 45° from normal (range = 2.68 to 9.87, n = 18; **Fig 3**). The close match between body transmission and non-coaxial eye reflectance further suggests gammarids could hide their eyes against any given background under most light environment scenarios.

Triplefin and gammarid eye size

From scaled pictures, we determined that triplefin pupil size averaged 0.78 mm (range 0.66 mm to 0.92 mm, n = 35 fish, one eye each) and the gammarid eye size averaged 0.0625 mm (range 0.0205 to 0.1020 mm, n = 11). Based on inter-photoreceptor distances measured from triplefin retinal mounts the visual acuity at the fovea is conservatively set around 6 cycles per degree, meaning that triplefins should be able to resolve the eye of the average gammarid eye from a distance of ~48 mm (23).

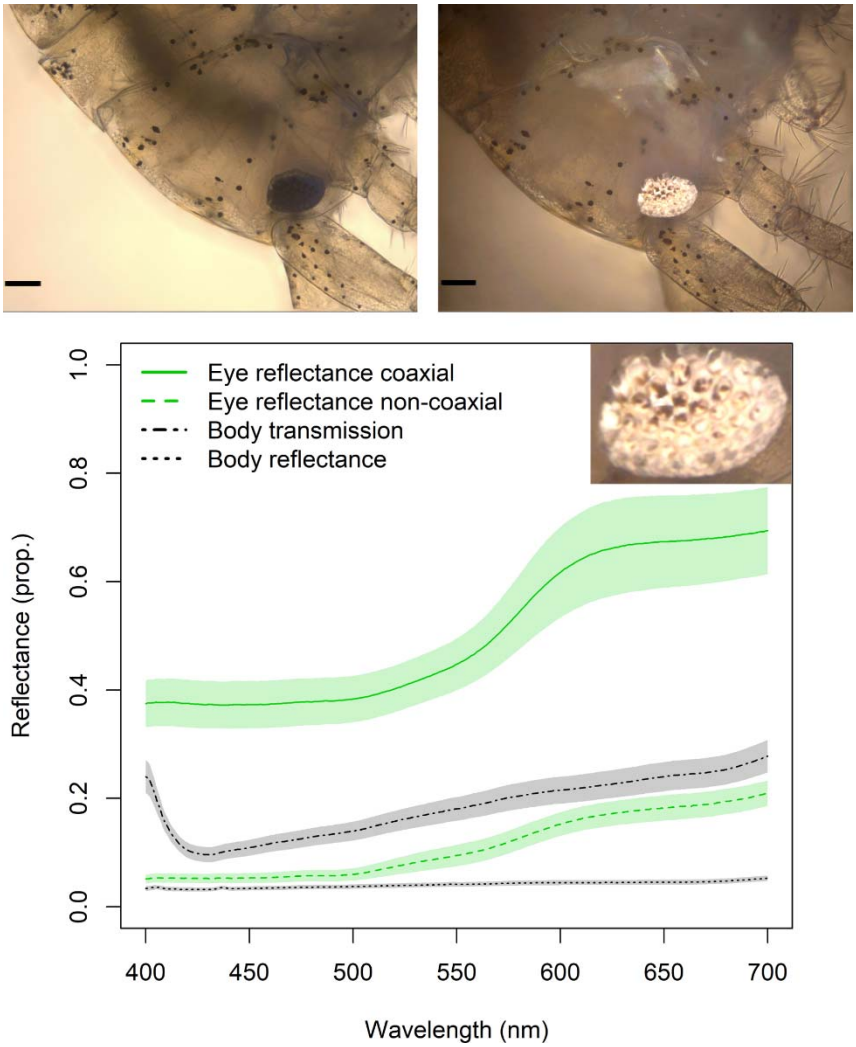

Figure 3. Top: Example gammarid for which measurements of body transmission and reflectance, as well as eye reflectance were obtained. Top left: viewed under 10 × 10 magnification using transmission illumination, scale bar is 100 µm; Top right: viewed with coaxial illumination, scale bar is 100 microns. Bottom: Reflectance and transmittance of the body (*n* = 19 individuals) and eye (*n* = 18 for coaxial and *n* = 10 for non-coaxial reflectance); lines indicate average of measurements, shaded area indicate standard error of the mean. Inset shows that the highly reflective structures are between ommatidia. Photo credit: Pierre-Paul Bitton.

Active photolocation of the gammarid eye

We compared the radiance of gammarid eyes as perceived by triplefins with and without the contribution of a blue ocular spark under various scenarios. Any change in radiance would allow the triplefin to detect potential prey items, e.g. by switching the ocular spark on and off, or when a mobile

prey changed the relative position of its eye. To explore the conditions suitable for diurnal active photolocation, we varied four parameters within observed ranges. These four were determined to affect active photolocation most strongly (see Methods). (1) **Spark size**: Because the photon flux that reaches the gammarid eye is directly related to the solid angle subtended by the ocular spark, we varied its radius equivalent on a continuous scale from 0.09 to 0.25 mm. (2) **Spark radiance**: The photon flux reaching the gammarid eye is also proportional to the relative radiance of the ocular spark so we varied it on a continuous scale from a mean area under the curve of 0.63 to 2.09. (3) **Gammarid eye reflectance:** The difference in gammarid eye radiance with and without the contribution of an ocular spark depends on the relationship between the reflective properties of the gammarid ocular reflectors under coaxial illumination and non-coaxial illumination. The non-coaxial component is used to estimate how bright the eye is under the prevailing conditions, without the addition of an ocular spark; the coaxial reflectance is used to calculate the contribution of the ocular spark to the total gammarid eye radiance. We evaluated the impact of the relationship between the coaxial and non-coaxial reflectance of gammarid ocular reflectors using three categories: large difference (non-coaxial reflectance is 9.87 times weaker than coaxial reflectance; maximum observed), average difference (4.09 times weaker), and small difference (2.68 times weaker; minimum observed). (4) **Shading of prey:** Finally, redirecting downwelling light into the horizontal plane would allow triplefins to generate greater contrasts with greater shading of prey, while the triplefin remains exposed to the same downwelling light. We investigated the influence of prey shading using four categories: no shade, weakly shaded, average shade, and strongly shaded (see Methods).

For each set of conditions, we calculated the maximum prey detection distance by means of active photolocation by calculating the chromatic and achromatic contrast between the gammarid eye with and without the radiance induced by a blue ocular spark as perceived by the triplefin at different distances (range 0.5 – 4.5 cm), and by comparing these values with specific chromatic and achromatic

149 contrast thresholds. The range of distances used is relevant to triplefin feeding behaviour, as it normally
150 targets prey items from one to three cm (personal observations). For chromatic contrast calculations we
151 used the receptor-noise limited model (24) parameterized using triplefin-specific visual characteristics
152 (20, 23), with a Weber fraction set at 0.05 (25, 26). For achromatic contrasts, we followed the
153 calculations in Siddiqi et al. (27) using a realistic Weber fraction of 0.02 (unpublished data; (28)), and a
154 conservative fraction of 0.05. To verify that the radiance from the ocular spark does not concurrently
155 change the luminance of the body of the gammarid, we also performed all calculations using body
156 transmittance and reflectance, assuming the gammarid was resting on the algal species *Halopteris*
157 *filicina*, a common triplefin foraging substrate (19).

158 Using a realistic Weber fraction of 0.02, the results from our models show that diurnal active
159 photolocation would assist with micro-prey foraging under wide ranging conditions (**Fig. 4**) by
160 generating perceivable achromatic contrasts in the eye of gammarids when modulating the ocular spark.
161 Chromatic contrast calculations did not yield values above six mm and are therefore considered
162 ineffective for gammarid detection using blue ocular sparks (results not shown). Neither achromatic nor
163 chromatic contrast calculations created perceivable contrasts on gammarid bodies (no detection
164 distance above five mm, results not shown). A conservative Weber fraction of 0.05 limited the
165 parameter space under which active photolocation based on achromatic contrasts would be beneficial
166 (**Fig. S1**), but demonstrated nonetheless the potential for ocular sparks to enhance prey detection at
167 distances relevant to triplefin foraging behaviour.

168 Under the most favourable conditions, the ocular spark could generate detectable achromatic
169 contrasts at 45 mm distance, the maximum modelled. This distance represents almost a full body length
170 of an average sized triplefin (29) and is much longer than the average striking distance (personal
171 observations: NKM, P-PB, MS, UKH). Under unfavourable parameter combinations, diurnal active
172 photolocation would generate perceivable achromatic contrasts at less than 10 mm, limiting its

potential to increase prey detection. In general, diurnal active photolocation would not be beneficial when triplefins forage on unshaded substrates (**Fig. 4** No shade). Under this scenario, only large and bright ocular sparks, and strong coaxial reflectance of gammarid eyes, would generate perceivable achromatic contrasts at distances > 10 mm. Even in poorly shaded areas, however, the ocular spark would generate perceivable contrast in the eye of gammarids at > 10 mm. When foraging on average or heavily-shaded substrate (**Fig. 4** third and fourth column), the distance at which active photolocation would be beneficial would greatly depend on the relationship between the coaxial and non-coaxial reflectance properties of the gammarid eyes. Under these shaded conditions, maximum detectable distances of over 15 mm would be common, suggesting diurnal active photolocation is effective in many situations. These results are in agreement with observations of triplefin foraging behaviour; they are often found feeding at small micro-habitat structures (e.g., complex algal growth, encrusting epi-growth, etc.).

The size of the ocular spark had a large effect on the model, simply because the amount of light striking the gammarid eye is strongly dependent on the perceived size of the spark from the gammarids' perspective. However, producing larger sparks may not be possible or beneficial. The evolution of the size of the reflecting chromatophore patch on which the spark is focused, and therefore the photon radiance available for active photolocation, is probably constrained by two factors. First, the maximum amount of light that can be directed towards the chromatophore is limited by the catchment area of the lens, which depends on the size, position and degree of protrusion through the pupil. This positioning is likely to be driven much more by regular vision than active photolocation. Second, *T. delaisi* is a crypto-benthic species which has evolved colour patterns particularly well suited for camouflage. Generating a large, highly visible spark could become a disadvantage if it attracted potential predators. Indeed, larger piscivorous fish are known to be attracted to brighter lures (30) and several such species are common in the same habitat (e.g. Fam. Serranidae).

197 The relationship between the coaxial and non-coaxial reflectance properties of the gammarid eye
198 also had much influence on the maximum detection distance. The reflectors, as those of stomatopod
199 larvae (12), are of unknown origin but are likely quarter-stack multilayers of dielectric material with
200 different refractive indices (11). As in other photonic crystals, such as 2D crystals (31, 32) and thin-films
201 (33), these particular reflectors usually have much stronger reflection at normal incidence. The
202 relationship between coaxial and non-coaxial reflectance could then be a function of the number of
203 layers, their spacing, and regularity.
204 Overall, our results describe how active photolocation through blue ocular sparks in the diurnal
205 triplefin *Tripterygion delaisi* could assist in the detection of prey items at relevant foraging distances.
206 Measurements of the red ocular spark (8) show that these are overall weaker, but may perhaps
207 generate a chromatic contrast in blue rich light environments, such as those found at the greater depths
208 of *T. delaisi*'s ecological range. We conclude that diurnal active photolocation by means of ocular sparks
209 can supplement regular vision by making the highly reflective eye of potential prey targets shine under
210 nearly-coaxial illumination. Given the high number of fish species that have both protruding lenses and
211 highly reflective irides, active photolocation could be widespread among fish, and an important, yet
212 previously disregarded, vision enhancement mechanism.
213

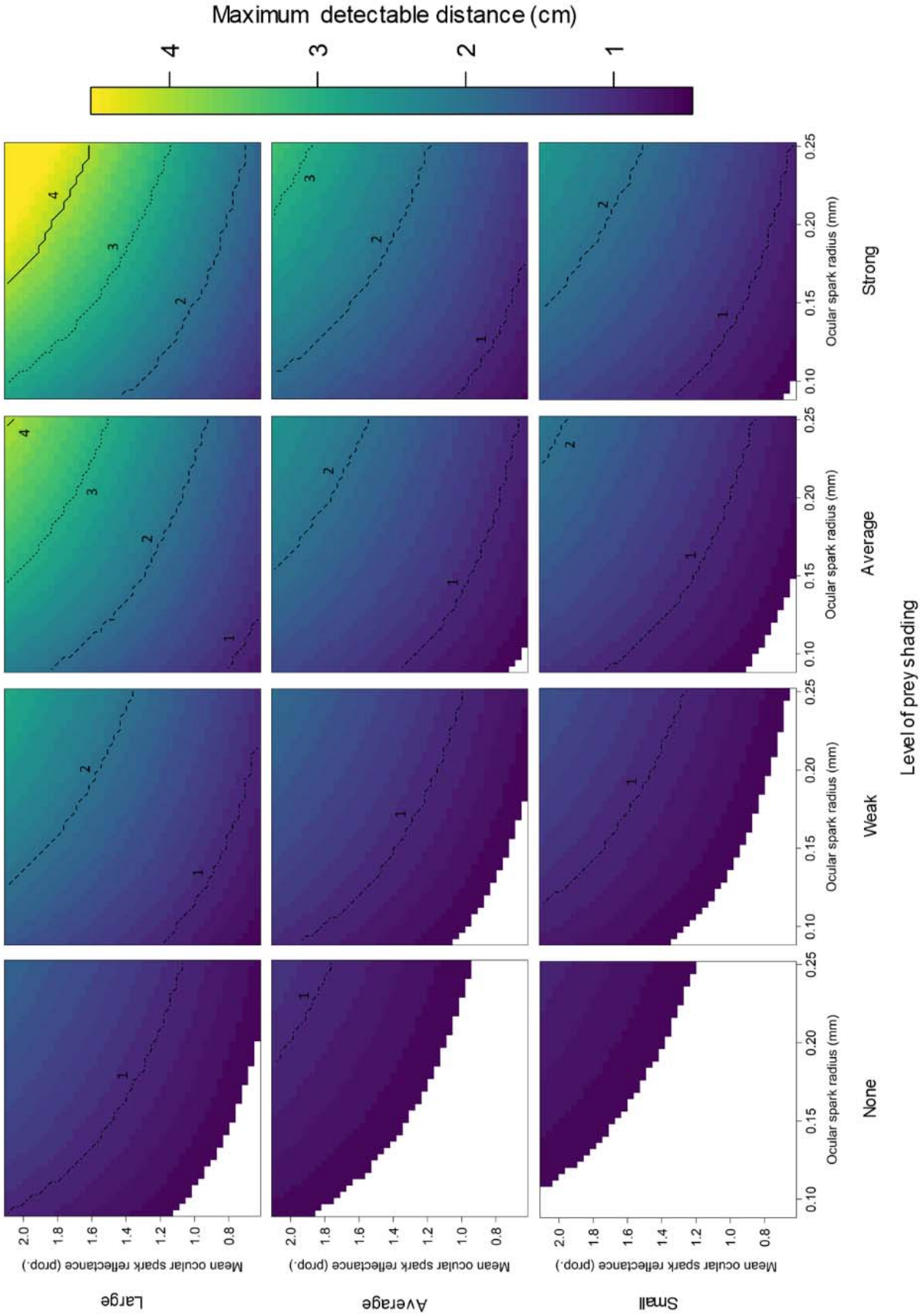

Figure 4. Maximum detection distances of the eye of gammarids by means of blue ocular spark reflectance under varying scenarios with Weber fraction set at 0.02. Top, middle, and bottom rows were obtained by varying the relationship between the reflectance of gammarid eyes with coaxial epi-illumination and at 45° from normal. Columns represent four scenarios of shading in which the prey item is located (See Material and Methods). Conditions in which active photolocation would not assist in gammarid detection are in white.

Materials and Methods

To determine whether ocular sparks produced by *Tripterygion delaisi* could generate a perceivable contrast in the eyes of gammarids, common triplefin prey items (18), we modelled interactions between prey and predator while varying influential parameters. The parameter space under which diurnal active pholocation may function was explored by (1) quantifying the downwelling and sidewelling light fields at various locations within *T. delaisi* ecological ranges, (2) measuring the reflective properties of the most common foraging substrate (*Halopteris filicina*), (3) measuring the size, and angle dependence of ocular sparks, and (4) measuring the optical properties of gammarid eyes and bodies. We combined these data to known properties of *T. delaisi*'s visual system (20) to calculate chromatic and achromatic contrast between the radiance of gammarid eyes as perceived by a *T. delaisi* individual with and without the radiance of its own blue ocular spark.

Ocular spark radiance

Radiance of the ocular spark was measured in live fish as described in Michiels et al. (8). To determine if the radiance of ocular sparks is equal in all directions, we collected angle-resolved measurements by securing whole triplefins, previously sacrificed by severing the spinal cord, in the center of a platform in a stainless steel hemisphere of 15 cm diameter placed on a PVC ring holder inside a 7 l Plexiglass® cylinder filled with fresh marine Ringer-solution. The reflective chromatophore patch responsible for generating the sparks was positioned at the exact center of the hemisphere, which was also the exact centre of cylinder, allowing measurements normal to the cylinder wall at all angles. Sparks were

generated by means of a stage lamp (ARRI® 650 Plus) mounted ~1.5 m above the fish. To avoid ambient light effects, the room was otherwise kept dark. For each of the 12 fish, the radiance of the ocular spark was measured with a Spectrascan PR-740 (PhotoResearch Inc., Syracuse, USA) fitted with a MLH-10X lens (Computar®) at each 10° between 10° (anteriorly) and 150° (posteriorly) in relation to the frontal-caudal axis of the fish's body (**Fig. 2**). The PR-740, uses Pritchard optics to collect measurements of absolute radiance of a specific solid angle, which is visualized as a small black circular area in the viewfinder. These values were expressed relative to the radiances of a polytetrafluorethylen (PTFE) diffuse white standard (Berghof Fluoroplastic Technology GmbH, Eningen unter Achalm, Germany) measured at the same angles and position immediately after each fish. The range of angles was not covered for all fish explaining why the sample size varied between angles (**Fig. 2**). Because the lens' resting state following death is slightly retracted, these measurements could only be used for comparing relative radiance at various angles as they underestimate spark intensity in relation to the illuminant. The size of the ocular spark was determined in 10 fish from scaled images analysed using ImageJ (34).

Gammarid spectroradiometry

Gammarids were isolated from *Halopteris filicina* algae collected between 5 and 10 m depth at STARESO (Calvi, Corsica), and immobilized but kept alive using a 0.6 M $MgCl_2$ solution. Spectral measurements were obtained with a PR-740 spectroradiometer mounted onto a Leica DM5000 B compound microscope (Leica Microsystems, Wetzlar, Germany) under 10 × 10 magnification. For reflectance measurements, we used an external halogen light source (KL2500 LCD, Schott AG, Mainz, Germany), either incident through the microscope's housing (epi-illumination) or at 45° to the sample using an external LLG 380 liquid light guide (Lumatec GMBH, Germany). For each gammarid we collected five body and eye reflectance measurements coaxially illuminated, and five measurements of eyes illuminated at 45°. We did not collect body reflectance at 45° because there was no evidence of coaxial

specularity or iridescence. The gammarid eye measurements were obtained from areas that covered almost the entire eye under 10 x 10 magnification. A submerged PTFE standard was also measured five times both with epi-illumination and with the light source at 45°. In all cases, the sample was repositioned and refocused before each measurement. Averages of 5 measurements of the body and eyes were expressed in relation to their relative standard. For transmission measurements we used the 12 V 100 W halogen lamp provided with the microscope in the transmitted light axis. For each gammarid, we took five radiance measurements of the transmitted light as seen through haphazardly selected locations on the body (plus Petri dish and $MgCl_2$ solution) and five measurements of the transmitted light without the gammarid (but including the Petri dish and $MgCl_2$ solution). Transmittance was then determined as the mean of the five measurements of the body divided by the reference. Scaled images of the gammarids were also obtained at this time and the size of the eyes subsequently estimated using ImageJ (34).

Field light environments and background reflectance

We measured the reflective properties of *Halopteris filicina*, a common foraging substrate for *T. delaisi*, and the downwelling light, unshaded sidewelling light, and shaded sidewelling light of triplefin habitat at the Station de Recherches Sous-marines et Océanographiques (STARESO) in Calvi (Corsica, France) in June-July 2014 and 2017. Details of *Halopteris filicina* data collection protocol can be found in Harant et al. (19). In short, substrate data were collected while scuba diving at a shallow site (5 m) characterized by rocky slopes, steep walls and granite boulders. Measurements were obtained at various locations in conjunction with a PTFE diffuse white standard (DWS) tilted at 45° to the surface as a combined measure of downwelling and sidewelling light. The relative radiance between the substrate measurements and light field is considered as the reflective property of *Halopteris filicina*. Light field measurements were instead obtained between 2 and 30 m depth on substrates facing south. At each

289 depth (2, 4, 6, 8, 10, 14, 18, 24, and 30 m) we measured from a 45° angle the radiance of an exposed
290 PTFE standard set at normal incidence to the water surface (= angle of incidence 0°) for an
291 approximation of downwelling light, and from a 90° a PTFE standard set at 90° to normal for measuring
292 sidewelling light, and a PTFE standard set at 90° to normal and shaded by a 4 cm opaque black cover as a
293 measure of shaded sidewelling light environment. Three measurements were obtained for every
294 standard at every depth and averages used in analyses. All measurements were obtained using a PR-740
295 fixed at a focal distance of 50 cm in a custom built underwater housing (BS Kinetics, Achern, Germany).
296 The PR-740 was equipped with a colour correction filter (#287 double CT orange, LEE Filters, Andover,
297 England) which suppresses, but does not block the dominant blue-green spectral range. This increases
298 exposure time, allowing the instrument to obtain better readings in the weak, long-wavelength part of
299 the spectrum at depth. Radiance measurements were corrected for the transmission profile of the filter
300 and port of the housing before being used in the calculations.
301
302 *Gammarid eye photon flux with and without ocular sparks*
303 We modeled a three-dimensional interaction between triplefins and gammarids, both on the same
304 horizontal plane, and assuming their eyes were positioned at normal incidence. We calculated the
305 photon flux of the reflective eye of the gammarid, as perceived by the triplefin, with and without the
306 contribution of the ocular spark, by describing the interaction in simple equations (see complete
307 calculation details in SI). In short, the photon flux of the gammarid eye without the contribution of the
308 spark reaching the triplefin retina was determined by the sidewelling light reflected by the ocular
309 reflectors (non-coaxial), the solid angle subtended by the gammarid eye (in steradians) as perceived by
310 the triplefin as a function of the distance between the two eyes, and the area of the triplefin pupil as the
311 ultimate receptor area (measured in ImageJ from scaled images (34)). The photon flux due to the ocular
312 spark returned to the triplefin was further determined by the radiance of the ocular spark, the solid

313 angle of the ocular spark (in steradians) from the perspective of the gammarid eye, and the coaxial
314 reflective properties of the gammarid's ocular reflectors. All solid angles were calculated using Monte
315 Carlo simulations (35).

316 In the model, we used fixed mean values for parameters that had little influence on the results,
317 based on preliminary sensitivity analyses. We set the gammarid eye radius at 0.0625 mm, the triplefin
318 pupil radius at 0.78 mm, used the downwelling light profile measured at 10 m, the mean background
319 substrate reflectance (*Halopteris filicina*), and the mean reflectance and transmittance of the gammarid
320 body. We explored the parameter space of the possible prey-predator interactions by varying the
321 factors that were determined to have the most influence on the contrast generated by the ocular spark
322 in the gammarid eye (parameter range and calculation details in Supplemental Information). We varied
323 the ocular spark radius measured in the laboratory (continuous range from 0.09 to 0.25 mm in intervals
324 of 0.004 mm), the ocular spark relative radiance (continuous from an area under the curve of 0.63 to
325 2.09 in relation to a white standard), the relationship between the coaxial and non-coaxial reflectance of
326 gammarid eyes (three categories: low difference based on the minimum observed, average difference
327 based on the measured mean, and large differences based on the maximum observed), and the
328 relationship between the downwelling and sidewelling light field (four categories: no shade, weakly
329 shaded, average shade, and strongly shaded). The 'no shade' was calculated as the average of the non-
330 shaded sidewelling light measurements divided by the average downwelling light, and the three shaded
331 categories were calculated as the minimum, average, and maximum observed shaded sidewelling light
332 measurements divided by the average downwelling light.

333 The spatial resolution of *T. delaisi* is conservatively estimated at 6 cycles/degree (23) which
334 means that the average gammarid eye diameter (0.125 mm) becomes a point source at ~48 mm. To
335 avoid modelling situations in which the gammarid eye is smaller than the smallest detectable point in
336 space by a triplefin, we limited the distance between the triplefin and the gammarid to a maximum of

337 45 mm. The minimum distance modelled relied on estimates of the distance of nearest focus (~5 mm;
338 based on calculations in (23)).
339
340 *Calculation of chromatic and achromatic contrasts*
341 Using retinal quantum catch estimations based on calculated photon flux, we calculated the differences
342 in chromatic and achromatic contrasts between the radiance of the gammarid eye with and without the
343 contribution of the ocular spark radiance. For the chromatic contrast we used the receptor-noise model
344 (Vorobyev and Osorio 1998), informed using the visual system characteristics of *T. delaisi* presented in
345 (20). In short, we used species specific ocular media transmission values, photoreceptor sensitivity
346 curves based on the single cone (peak at 468 nm), and the double cone (peaks at 517 and 530 nm)
347 following a vertebrate photoreceptor-template (36), and a relative photoreceptor density of single to
348 double cones set at 1:4 as found in the triplefin fovea (23). Since the Weber fraction (ω) for colour
349 contrast is not known for fish, we used a value of 0.05 as in previous studies from other groups (25, 26).
350 We calculated the achromatic contrast as $\log(Q_1/Q_2)/\omega$, where Q_1 and Q_2 are the quantum catches of
351 the two members of the double cones which are associated with the achromatic channel, under photon
352 flux_1 and photon flux_2 respectively (27). We used two different Weber fractions for our calculations: a
353 conservative value for fish (ω = 0.05) according to work conducted on *Carassius auratus* (Hester 1968),
354 *Scardinius erythrophthalmus* (37), *Gadus morhua* (38), and *Lepomis machrochirus* (39), and the mean
355 value of these studies (ω = 0.02 (28)). Recent work by our unit confirmed that triplefins have contrast
356 sensitivity at or below ω = 0.02 (in prep.). Since this parameter is extremely influential in the calculation
357 of contrasts (40, 41), and one of the Weber fractions selected is conservative, our achromatic contrast
358 values also include conservative estimates. Both calculations of chromatic and achromatic contrast
359 result in measures of just-noticeable differences (JNDs), where values above one are considered to
360 represent the minimum discernable differences between the quantum catches. To ensure that the

361 contrast generated by the ocular spark was only influencing the radiance of the gammarid eye and not
362 the background, we performed the same calculations but for the gammarid body.
363
364 *Calculation of maximum discernable distance*
365 For each set of model conditions defined in the section *Gammarid eye photon flux with and without*
366 *ocular sparks*, we determined the maximum discernable distance of the ocular spark radiance returned
367 by the gammarid eye. This was achieved by calculating the chromatic and achromatic contrast at each
368 millimeter between 5 and 45 mm per set of conditions, and extracting the first value at which the
369 contrast was equal to or exceeding 1.0 JND (**Fig. S2**).
370
371 *Animal care and permits*
372 Fish were caught at STARESO between 5 and 20 m depth using hand nets while scuba diving. During
373 dives, fish were transported in 50 ml perforated Falcon™ tubes (Corning Inc, NY, USA) to permit water
374 exchange. At the field station the fish were held in a 50 L flow-through tank at ambient water
375 temperature, until transferred to facilities at the University of Tübingen, Germany. In these facilities,
376 individuals were kept separately in 15 L flow-through tanks (18°C, salinity 34‰, pH 8.2, 12 L: 12 D light
377 cycle) and fed once per day. The fish were sacrificed under permit 'Mitteilung 29.10.2014' from the
378 Regierungspräsidium (Referat 35, Konrad-Adenauer-Str. 20, 72072 Tübingen) under the supervision of
379 the animal welfare officer. We captured triplefins in STARESO under the station's general scientific
380 permit.
381
382 **Acknowledgements**
383 We thank the staff at STARESO, especially Corrine Pelaprat for assistance with identification of
384 gammarids, and Oeli Oelkrug for fish maintenance at the University of Tuebingen. This project was

385 funded by the German Science Foundation Koselleck grant (Mi482/13-1) and the Volkswagen
386 Foundation (Az. 89148 and Az. 91816) to N.K.M. as well as running support by the University of
387 Tübingen. P-P.B. was funded by the Natural Sciences and Engineering Research Council of Canada in the
388 form of a Postdoctoral Fellowship.

389

390 *Data Archival*

391 All data and R scripts used in the analyses and preparation of figures will be made available on Dryad
392 upon acceptance, and are available to the editors and reviewers during the evaluation process.

393 *References*

394 1. Pierce GW & Griffin DR (1938) Experimental determination of supersonic notes emitted by bats.
395 *Journal of Mammalogy* 19:454-455.
396 2. Griffin DR, Webster FA, & Michael CR (1960) The echolocation of flying insects by bats. *Anim*
397 *Behav* 8:141--154.
398 3. Caputi AA & Budelli R (2006) Peripheral electrosensory imaging by weakly electric fish. *J Comp*
399 *Physiol A* 192(6):587-600.
400 4. Rasnow B (1996) The effects of simple objects on the electric field of Apteronotus. *Journal of*
401 *Comparative Physiology a-Sensory Neural and Behavioral Physiology* 178(3):397-411.
402 5. Kenaley CP, DeVaney SC, & Fjeran TT (2014) The Complex Evolutionary History of Seeing Red:
403 Molecular Phylogeny and the Evolution of an Adaptive Visual System in Deep-Sea Dragonfishes
404 (Stomiiformes: Stomiidae). *Evolution* 68(4):996-1013.
405 6. Hellinger J*, et al.* (2017) The flashlight fish Anomalops katoptron uses bioluminescent light to
406 detect prey in the dark. *Plos One* 12(2):e0170489.
407 7. Sutton TT (2005) Trophic ecology of the deep-sea fish Malacosteus niger (Pisces : Stomiidae): An
408 enigmatic feeding ecology to facilitate a unique visual system? *Deep-Sea Res Pt I* 52(11):2065-
409 2076.
410 8. Michiels NK*, et al.* (2018) Controlled ocular radiance in a diurnal fish looking at prey. *Royal*
411 *Society Open Science* 5:170838.
412 9. Johnsen S (2012) *The optics of life : a biologist's guide to light in nature* (Princeton University
413 Press, Princeton, NJ) pp x, 336 p., 338 p. of plates.
414 10. Marshall J & Johnsen S (2017) Fluorescence as a means of colour signal enhancement. *Philos T R*
415 *Soc B* 372(1724).
416 11. Land MF & Nilsson D-E (2012) *Animal eyes* (Oxford University Press, Oxford ; New York) 2nd Ed
417 pp xiii, 271 p., 274 p. of plates.
418 12. Feller KD & Cronin TW (2014) Hiding opaque eyes in transparent organisms: a potential role for
419 larval eyeshine in stomatopod crustaceans. *J Exp Biol* 217(18):3263-3273.
420 13. Land MF (1972) The physics and biology of animal reflectors. *Progress in biophysics and*
421 *molecular biology* 24:75-106.
422 14. Santon M, Bitton P-P, Harant UK, & Michiels NK (In Press) Daytime eyeshine contributes to pupil
423 camouflage in a cryptobenthic marine fish. *Sci Rep-Uk*.
424 15. Shelton PMJ, Gaten E, & Herring PJ (1992) Adaptations of Tapeta in the Eyes of Mesopelagic
425 Decapod Shrimps to Match the Oceanic Irradiance Distribution. *J Mar Biol Assoc Uk* 72(1):77-88.
426 16. Howland HC, Murphy CJ, & Mccosker JE (1992) Detection of Eyeshine by Flashlight Fishes of the
427 Family Anomalopidae. *Vision Res* 32(4):765-769.
428 17. Nicol JAC (1960) Spectral composition of the light of the lantern-fish, Myctophum punctatum. *J*
429 *Mar Biol Assoc Uk* 39:27-32.
430 18. Zander CD (1982) Feeding ecology of littoral gobiid and blennioid fish of the Banyuls area
431 (Mediterranean Sea) I. Main food and trophic dimension of niche and ecotope. *Vie et Milieu*
432 32:1-10.
433 19. Harant UK*, et al.* (In Press) Do the fluorescent red eyes in the marine fish Tripterygion delaisi
434 stand out? In situ and in vivo measurements at two depths. *Ecology and Evolution*.
435 20. Bitton PP*, et al.* (2017) Red fluorescence of the triplefin Tripterygion delaisi is increasingly visible
436 against background light with increasing depth. *Royal Society Open Science* 4(3):161009.
437 21. Nelson ME & MacIver MA (2006) Sensory acquisition in active sensing systems. *J Comp Physiol A*
438 192(6):573-586.

22. Fritsch R, Ullmann JFP, Bitton PP, Collin SP, & Michiels NK (2017) Optic-nerve-transmitted eyeshine, a new type of light emission from fish eyes. *Frontiers in Zoology* 14.
23. Fritsch R, Collin SP, & Michiels NK (2017) Anatomical Analysis of the Retinal Specializations to a Crypto-Benthic, Micro-Predatory Lifestyle in the Mediterranean Triplefin Blenny Tripterygion delaisi. *Front Neuroanat* 11.
24. Vorobyev M & Osorio D (1998) Receptor noise as a determinant of colour thresholds. *P Roy Soc B-Biol Sci* 265(1394):351-358.
25. Matz MV, Marshall NJ, & Vorobyev M (2006) Are corals colorful? *Photochemistry and Photobiology* 82:345-350.
26. Wilkins L, Marshall NJ, Johnsen S, & Osorio D (2016) Modelling fish colour constancy, and the implications for vision and signalling in water. *J Exp Biol*:jeb-139147.
27. Siddiqi A, Cronin TW, Loew ER, Vorobyev M, & Summers K (2004) Interspecific and intraspecific views of color signals in the strawberry poison frog *Dendrobates pumilio*. *J Exp Biol* 207(14):2471-2485.
28. Douglas RH & Hawryshyn CW (1990) Behavioural studies of fish vision: an analysis of visual capabilities. *The visual system of fish*, eds Douglas RH & Djamgoz MBA (Chapman Hall, London, UK), pp 373-418.
29. De Jonge J & Videler JJ (1989) Differences between the Reproductive Biologies of Tripterygion-Tripteronotus and Tripterygion-Delaisi (Pisces, Perciformes, Tripterygiidae) - the Adaptive Significance of an Alternative Mating Strategy and a Red Instead of a Yellow Nuptial Color. *Mar Biol* 100(4):431-437.
30. Moraga AD, Wilson ADM, & Cooke SJ (2015) Does lure colour influence catch per unit effort, fish capture size and hooking injury in angled largemouth bass? *Fish Res* 172:1-6.
31. Eliason CM, Bitton PP, & Shawkey MD (2013) How hollow melanosomes affect iridescent colour production in birds. *P Roy Soc B-Biol Sci* 280(1767).
32. Meadows MG, Morehouse NI, Rutowski RL, Douglas JM, & McGraw KJ (2011) Quantifying iridescent coloration in animals: a method for improving repeatability. *Behav Ecol Sociobiol* 65(6):1317-1327.
33. Van Wijk S, Belisle M, Garant D, & Pelletier F (2016) A reliable technique to quantify the individual variability of iridescent coloration in birds. *J Avian Biol* 47(2):227-234.
34. Abràmoff MD, Magalhães PJ, & Ram SJ (2004) Image processing with ImageJ. *Biophotonics International* 11(7):36-42.
35. Whitcher R (2006) A Monte Carlo method to calculate the average solid angle subtended by a right cylinder to a source that is circular or rectangular, plane or thick, at any position and orientation. *Radiation protection dosimetry* 118(4):459-474.
36. Govardovskii VI, Fyhrquist N, Reuter T, Kuzmin DG, & Donner K (2000) In search of the visual pigment template. *Visual Neurosci* 17(4):509-528.
37. Muntz WRA & Northmore DPM (1970) Vision and visual pigments in a ish, Scardinius erythrophthalmus (Rudd). *Vision Res* 10(4):281-298.
38. Anthony PD (1981) Visual contrast thresholds in the cod Gadus morhua L. *J Fish Biol* 19(1):87-103.
39. Hawryshyn CW, Arnold MG, Mcfarland WN, & Loew ER (1988) Aspects of color-vision in Bluegill sunfish (Lepomis macrochirus) - Ecological and evolutionary relevance. *Journal of Comparative Physiology a-Sensory Neural and Behavioral Physiology* 164(1):107-116.
40. Bitton PP, Janisse K, & Doucet SM (2017) Assessing sexual dicromatism: The importance of proper parameterization in tetrachromatic visual models. *Plos One* 12(1):e0169810.
41. Olsson P, Lind O, Kelber A, & Simmons LW (2017) Chromatic and achromatic vision: parameter choice and limitations for reliable model predictions. *Behav Ecol*:arx133.

Supplemental Information

Table S1. Symbols used in the equations to calculate the photon flux of the gammarid eye reaching the triplefin, with and without the contribution of the ocular spark

Symbol	***Definition***
L	Photon radiance (photons s^{-1} sr^{-1} m^{-2})
S	Blue ocular spark relative radiance (proportion of a PTFE white standard)
d	Distance between triplefin and gammarid eyes (m)
r_t	Radius of triplefin pupil (m)
R_{ca}	Reflectance of gammarid eye (coaxial) (proportion of a PTFE white standard)
R_{nca}	Reflectance of gammarid eye (non-coaxial) (proportion of a PTFE white standard)
Φ	Photon flux coming from the gammarid eye reaching the triplefin pupil (photons s^{-1})
Ω	Solid angle of target as perceived by receiver (sr)

Photon flux calculations

We calculated the photon flux of the gammarid eye reaching the triplefin pupil with and without the radiance of the ocular spark, assuming that the center of the triplefin pupil was at normal incidence to the center of the eye of the gammarid, i.e. the full area of the pupil of the triplefin is visible to the gammarid and vice versa. We also assume the effect of absorbance and scattering of the water to be negligible since all energy transfers occur over distances shorter than 5 cm.

Photon flux without ocular spark

The base photon radiance of the gammarid eye (L_0) is a function of the sidewelling light field (L_{sw}) and the reflectance of the gammarid eye with non-coaxial illumination:

$$L_0 = L_{sw} \times R_{nca} \quad (1)$$

The photon flux reaching the retina of the triplefin without the ocular spark (Φ_{ns}) is the proportion the gammarid radiance multiplied by the solid angle of the gammarid eye (Ω_{gam}) and the area of the triplefin pupil (πr_t^2):

$$\Phi_{ns} = L_0 \times \Omega_{gam} \times \pi r_t^2 \quad (2)$$

Photon flux produced by ocular spark

The photon radiance of the ocular spark (L_{os}) is a determined by the downwelling light field (L_{dw}), the catchment area of the lens, and the reflective properties of the iris chromatophores on which the light is focused. The effect of the lens and reflective properties of the chromatophores have only been measured together and are treated as a relative radiance value (S).

$$L_{os} = L_{dw} \times S \quad (3)$$

The radiance of the gammarid eye (L_{gam}) caused by the reflection of the ocular spark is estimated by multiplying the radiance of the ocular spark reaching the gammarid (L_{os}) with the solid angle of the ocular spark (Ω_{os}) and the reflectance of the gammarid eye with illumination coaxial to the receiver (R_{ca}). Because the properties of the gammarid eye are measured in relation to a diffuse white standard, the photon exitance from the gammarid eye is converted to photon radiance by dividing by π steradians:

$$L_{gam} = L_{os} \times \Omega_{os} \times R_{ca} \times \pi^{-1} \quad (4)$$

The photon flux generated by the ocular spark which reaches the triplefin retina (Φ_{os}) is determined as the proportion of the ocular spark generated gammarid eye radiance (Eq. 4) multiplied by the perceived size of the gammarid eye, in steradians, and the area of the triplefin pupil:

$$\Phi_{os} = L_{os} \times \Omega_{os} \times R_{ca} \times \pi^{-1} \times \Omega_{gam} \times \pi r_t^2 \quad (5)$$

The total photon flux reaching the retina of the triplefin with the ocular spark is then the sum of equations (2) and (5).

A similar calculation was used for the effect of the ocular spark on the illumination of the gammarid body. In these calculations we estimated the photon flux reaching the retina of the triplefin with and without the contribution of the ocular spark, using the same solid angles. In contrast to calculations with the gammarid eye, we used the same body reflectance values for the coaxially and non-coaxially illuminated scenarios. The photon exitance from the body, both with and without the contribution of the ocular spark was determined as the proportion of light that was reflected by the body and the proportion of light that was transmitted through the body, reflected by the substrate, and transmitted again through the body.

For all calculations, the solid angle of the gammarid eye from the perspective of the triplefin pupil (Ω_{gam}), and the solid angle of the ocular spark from the perspective of the gammaridh eye (Ω_{os}), in steradians, were estimated by Monte Carlo simulation (35). The triplefin pupil, gammarid eye, and ocular spark were treated as disks of zero thickness. The pupil and gammarid eye were always positioned centered and at normal incidence to one another, and the ocular spark positioned at the edge of the iris (displacement = 1.09 mm) in the same plane and normal vector as the triplefin pupil. Because we estimate that the triplefin can focus on objects minimally at 7 mm and that average gammarid eye becomes a point source beyond ~48 mm, we determined the solid angles for distances between 5 mm and 45 mm. The calculations were based on 1E09 photon packets emitted from the source; these generated solid angle estimates with 99.9% confidence intervals with errors ranging from 1.2 % of the solid angle value at 5 mm to 10.6 % at 45 mm.

Exploration of parameter space

To explore the parameter space of our interaction between triplefins and gammarids, we varied the parameters known to have the most influence on the calculated contrasts. To allow comparison and visualization of the results, we chose to model two continuous parameters: ocular spark radius, and the ocular spark relative radiance, and two categorical parameters: the relationship between the coaxial and non-coaxial reflectance of the gammarid eyes, and the relationship between the downwelling and sidewelling light field.

The parameter 'ocular spark radius' ranged from 0.09 mm to 0.25 mm (based on actual measurements ranging from 0.10 mm to 0.24 mm) in 41 intervals of equal increments (0.004 mm). The range values for the parameter 'ocular spark relative radiance' was produced by first taking the mean value of all measurements at each wavelength (binned in 1 nm interval) and varying the area under the curve between the measured range of 63 % to 209 %. To produce square matrices of results, the value range was also divided in 41 intervals of equal increments.

The relationship between the coaxial and non-coaxial reflectance of gammarid eyes was not correlated in the samples measured. To explore the influence of this parameter we calculated the average difference between the coaxial and non-coaxial eye reflectance measurement obtained from each gammarid, calculated at each wavelength (binned in 1 nm interval), and varied the area under the curve to represent the minimum value observed (10.1 %), the average value (24.4%), and the maximum value observed (37.25 %).

572 We included four measures of the relationship between the downwelling and sidewelling light
573 fields: no shade, weakly shaded, average shade, and strongly shaded. The relationship between the
574 downwelling and unshaded sidewelling spectral light profile was obtained by taking their ratio at several
575 measured locations. The three categories of shaded sidewelling light were obtained by calculating the
576 average difference between the downwelling and shaded sidewelling light fields at each measurement
577 station, and varying the area under the curve to represent the minimum value observed (ratio DW/SW =
578 8.65), the average value (ratio = 16.62), and the maximum value observed (ratio = 26.63). These
579 conversion vectors were then applied to the downwelling light field obtained at 10 m depth.
580

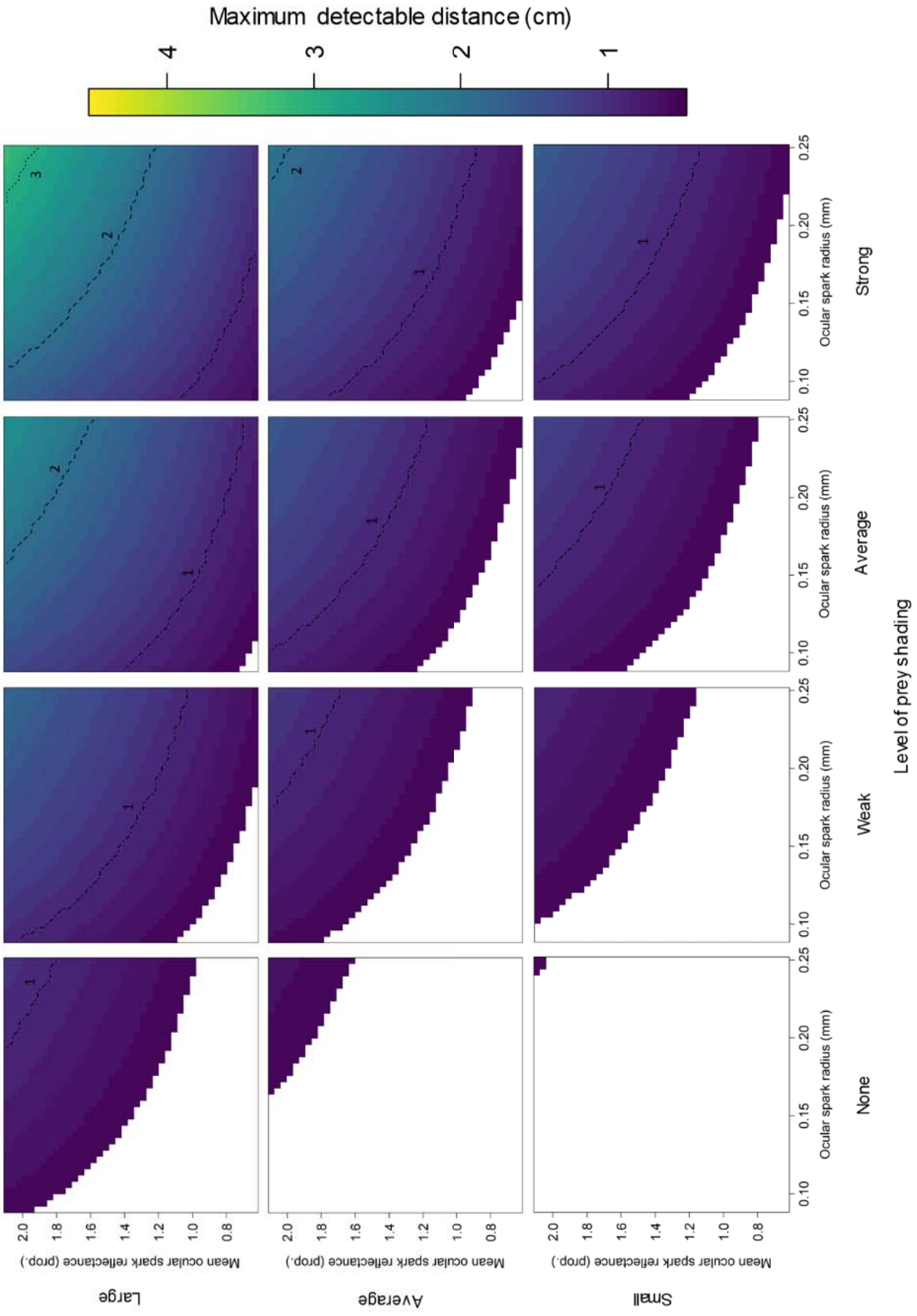

582 **Figure S1.** Maximum detectable distances of ocular spark reflectance from the eye of gammarids under varying
583 scenarios (Weber fraction = 0.05). Top, middle, and bottom row were obtained by varying the relationship
584 between the reflectance of gammarid eyes with coaxial epi-illumination and at 45° from normal. Vertical rows
585 were obtained by varying the amount of shade on which prey items rests. Conditions in which active photolocation
586 would not assist in gammarid detection are in white.
587

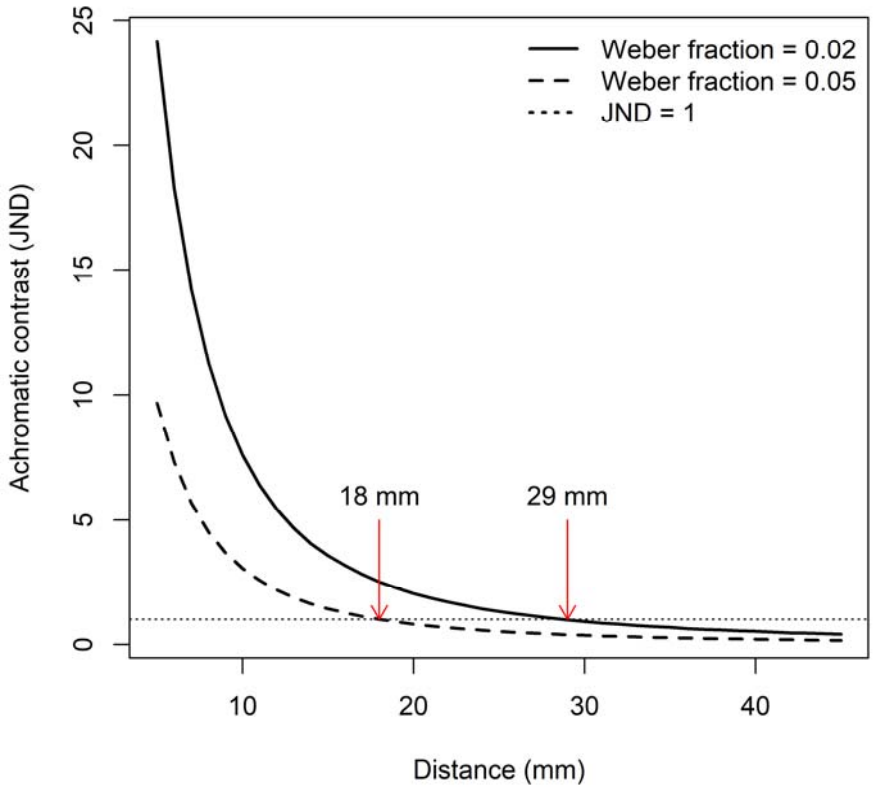

588

589 **Figure S2.** Example extrapolation of the maximum distance at which reflections in the gammarid eye caused by
590 ocular spark radiance are discernable. The achromatic contrast is the perceived difference in photon flux from the
591 gammarid eye with and without ocular spark contribution. The maximum discernable distance is defined as the
592 distance at which the contrast is equal to one just-noticeable-difference (JND). All calculations were repeated
593 twice, once with the Weber fraction set at 0.05, once with the Weber fraction set at 0.02 (See Material and
594 Methods).
595